Spring 2024

Cost-effective PV Panel Back Mount for Temperature Control and Heat Utilization

Jiuning Ren , '24

Cost-effective PV Panel Back Mount for Temperature Control and Heat Utilization

Jiuning Ren

Engineering Department

Swarthmore College

4/26/2024

Abstract

The efficiency of a PV panel is limited by its temperature, where panel efficiency drops with increasing operating temperature, resulting in low panel efficiency in hot summers. This project aims to design and implement a cheap and efficient cooling system for a PV panel in the form of a panel back mount. For this project, Solar Lab facilities were updated and used as systems for testing the functionalities of the back-panel mount design. These facilities include a Q.PEAK DUO BLK-G8+ 340 Monocrystalline silicon module PV panel, a Prostar PS-15M solar charge controller for power maximization and PV panel power monitoring, a Seahawk deepcycle battery as a load for the panel output, and a solar thermal fluid circulation and data acquisition system consisting of various pumps, valves, and sensors. Testing was done on a sunny, cloudless, and warm day in late April.

The results show that the system operating at a relatively low temperature and small temperature difference, with a maximum panel temperature of less than 41℃ and a maximum panel temperature drop of 6 ℃, starts to experience a significant decrease in PV panel temperature and induce a reasonable increase in electrical output of around 20 Watts. Because of relatively cool ambient temperatures, the effectiveness of the heat transfer is not as large as estimated, and more experiments are recommended during mid-summer for a better understanding of the system. Future efforts should focus on increasing the thermal contact area, downsizing the system, and closing the circulation loop to generate conclusive results on system efficiency and cost-benefit evaluation.

1. Introduction

Anthropogenic climate change has become one of the most prominent issues in the modern world. Various efforts have been put forth toward sustainable energy generation. Among these, photovoltaic panels are considered green alternative energy sources, as they do not produce greenhouse gas emissions during energy generation. The ease of installment and flexibility in scale have made solar photovoltaic panels prevalent sustainable electricity generation options.

To understand the dynamics of photovoltaic panels and their interactions with the ambient, one must first look at the basic principles of this technology. A photovoltaic panel consists of many photovoltaic cells, or PN junctions of semiconducting material, connected

metallically in series and parallel. The net current of cells connected in parallel is the sum of the current of each cell, and the net voltage of cells connected in series is the sum of voltages, accordingly. The term photovoltaic refers to the cell's utilization of the photoelectric effect, where incoming photons strike the surface of the semiconducting materials, exciting charge carriers from the valence band to the conduction band, where they are allowed to move under the effect of drift, diffusion, generation, and recombination that are the properties of junctions of p-type and n-type semiconductor materials.

In a PN junction of the photovoltaic cell, a depletion region is formed between the p-type and n-type doped materials due to the diffusion of carriers into the oppositely charged region. These diffusions leave behind oppositely charged donor or acceptor atoms (electron diffusion leaving behind positively charged atoms and hole diffusion leaving behind negatively charged ones) that create an electric field to prevent further diffusion, creating a region of depletion that carriers cannot cross under equilibrium. Hence, the excited carriers are forced to flow across the load connected through the wiring and the metallic connections on either end of the semiconducting material. A continued flow of current is thus formed that provides electrical power to the load, which is never depleted as the system is in dynamic equilibrium. Diagrams of the photovoltaic cell and the PN junction are shown in Fig. 1.

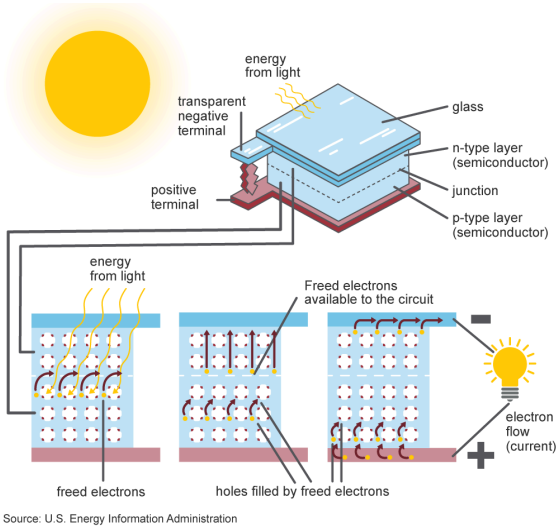

(a)

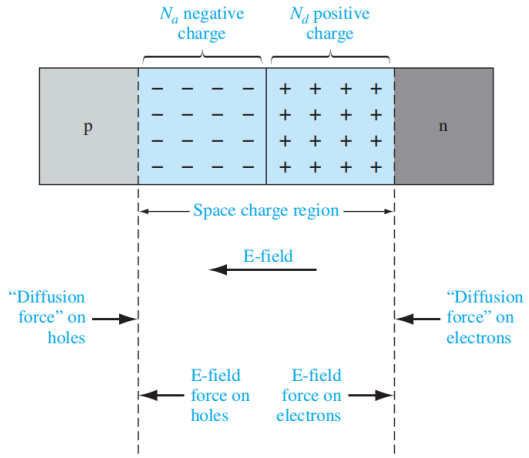

(b)

Figure 1. (a) photovoltaic cell[1] and (b) PN junction.[2]

A common issue facing most commercial photovoltaic panels is low energy efficiency. Most commercial solar panels have efficiencies ranging from 17% to 20%.[3] Excess heat brought by the incoming photons could exacerbate this problem significantly. Photons that have energies higher than needed for carriers to cross the bandgap pass on the energy to carriers, and the energy is released as waste heat as carriers settle back into the valence band. This leads to higher carrier mobility and recombination losses and causes fewer carriers to produce electrical power. In practice, panel efficiency drops with increasing operating temperature at a rate of −0.5%/°C.[4] As shown in Fig. 2, the efficiency of the PV panel rises nearly linearly with the drop in temperature. However, economic and energy use considerations make it more viable to determine an operating temperature near room temperature, in which the PV panel could produce a net positive output.

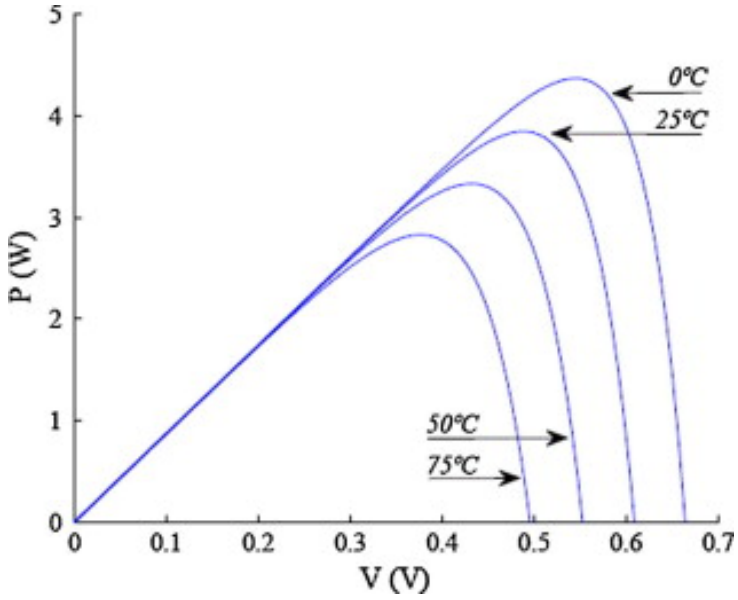

Figure 2. PV panel power and voltage relationship to different temperatures.

[1] (Neamen, Donald)
[2] ("Photovoltaics and Electricity")
[3] ("Photovoltaic Energy Factsheet")
[4] (Moharram et al.)

Due to the reasons above, it is worthwhile to investigate whether there is a method for cooling PV panels to allow a net increase in power output. Furthermore, for individual households that possess one or two panels, the method should be cost-effective to make it economical to increase the net power output. In other words, there should be a net positive change in power output over the panel price. For this purpose, this project is focused on developing a hybrid PV-thermal panel by introducing a cost-effective mount on the back of an existing PV panel. A hybrid panel uses some thermal circulation fluid put into thermal contact with the panel to cool it and gather the waste heat of the panel to be used elsewhere for purposes such as pre-heating domestic hot water. The cooling process of hybrid panels is well-established, and materials can be easily accessible and cheap to manufacture. These advantages make hybrid panels suitable for the proposed objective, although various disadvantages including the requirement of energy input (for circulation pumps and possible chiller for cooling circulation fluids) and the efficiency's dependence on ambient temperature limit the applications of hybrid panels. Hence, it is important to find a middle point between the benefits and drawbacks to meet the goal of this project.

2. Technical Discussion

My research project on validating hybrid PV-thermal panels in the summer of 2022 showed an approximately 30 ℃ drop in the surface temperature of a PV panel when it was put into thermal contact with flowing room-temperature water with a mass flow rate of approximately 30 grams per second, resulting a rise of the PV panel's maximum power efficiency from 15% to 17.5%, which roughly indicates a 40-watt rise in panel electrical power output. The process also generated a 3 to 5 ℃ rise in the flowing water. The process utilized direct flow, and water directly flowed onto the panel via drip holes in a pipe and was collected at the bottom. A graph of the measured rise in PV panel efficiency is reproduced in Fig. 3.

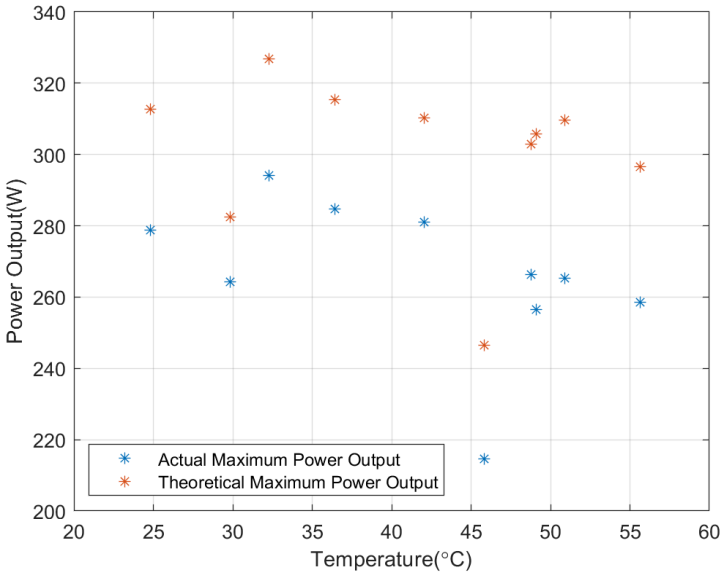

Figure 3. Power output decreases with increasing temperature.

The end goals for this project consisted of multiple parts. A primary goal for this project was to ensure that the system results in a net increase in power output for the PV panel. The power output of a PV panel can be predicted by a model of five equations summarized in Chapter 23, *Solar Engineering of Thermal Processes, Photovoltaics and Wind* ("Design of Photovoltaic Systems" pp. 762)[5], where a series of current-voltage relationships can be determined based on temperature differences. Realistic results can be compared to this model to assess the accuracy and performance of the panel. However, due to limitations of the results collected as will be discussed in the Discussions section, this verification is beyond the scope of this report.

A secondary goal was an efficient heat transfer between the panel and the attachment. A proposed metric for this goal is the ratio between the rate at which heat is delivered to the circulating fluid and the power of the solar irradiance received by the panel, as shown in Eq. 1,

$$\eta_{ht} = \frac{P}{W} \tag{1}$$

where η_{ht} represents the metric for the efficiency of heat transfer, W is the power of the solar irradiance or the irradiance multiplied by the area of the panel, and P represents the rate at which heat is transferred to the circulating fluid,

[5] (Duffie, John A., et al.)

$$P = \dot{m} c_p \Delta T \quad (2)$$

These end goals were separated into four categories:

1. Cooling. Designs and materials were chosen to produce good thermal conductivity to allow heat transfer from the back of the panel to the circulation fluids flowing within the channels of the back attachment.
2. Temperature control. Electronics and codes were assembled to collect temperature and flow rate data from the back attachment and modify the flow rate and/or temperature of the circulating fluid to maintain an optimal operating temperature.
3. Electrical efficiency. The electrical power output of the PV panel was easily accessible through its power regulating system, and the power consumption of the circulation system was expected to be as low as possible. Previous experiments showed a rise in power with an average of 40 W.
4. Thermal efficiency. Materials with good insulation were chosen to prevent heat from dissipating during the heat transfer process. Thermocouples attached at the inlet and outlet of the attachment collected temperature information to compare with solar irradiance data measured by a pyranometer mounted on the PV panel.

2.1 Design Goals

To accomplish the end goals stated before, the following design goals and specifications were made:

1. η_{ht} should be greater than 0.25. Previous experiments in summer showed that it was possible to achieve a minimum of 678 W rise in thermal power of the circulating water with an approximately 1900 W solar irradiance, corresponding to a minimum of 3 ℃ rise in circulating water temperature. Considering the lessened power of the pump and the reduced efficient thermal contact, 0.25 should be an acceptable metric for heat transfer.
2. The temperature of the panel surface should be within the range of 25 ± 2 ℃ during cooling to obtain optimum operating temperatures.

3. The power consumption of sensors and the microcontroller should be maintained below 5 W. The power consumption of the pump should be below 30 W.

2. Methods

To achieve the stated goals, measures, and testing mechanisms were developed to implement and assess designs.

2.1 Implementation and Testing Process

The initial phase of the project included learning the revamped fluid circulation system that switched from using Programmable Logical Controller control to an NI USB-6003 DAQ-based control box with a MATLAB interface. Different system parts were calibrated, including the flowmeter, pumps, valves, and temperature sensors. Codes were developed for automated control of the system. An example code is included in Appendix I, which details the procedures for system startup, various running statuses of the system with different valve configurations, and data acquisition for temperature and flow rate. With the solar thermal and PV monitoring systems in place, all required data can be derived from flow rate, temperature data, and panel output power collected by the systems. The design of the cooling apparatus was implemented, and the collected data was processed to obtain the parameters to be compared to the design goals.

2.2 Mount and Related System Design

The main structure of the mount was implemented with ¾ inch-diameter soft copper tubing material. The entire structure used a raster-scan pattern that allowed a single flow of fluid to cover most of the panel surface. Generic soft copper tubing was purchased and bent to a repeating s-shape with a bending tool.

Figure 4. Bent copper tubing along the back of the PV panel.

The structure is supported by existing Unistrut beams along the back of the panel with additions to ensure the fullest contact between the mount and the panel. The inlet PEX tubing is connected to the lower end of the copper tubing, and the outlet of the copper tubing is connected to the PEX tubing that returns water to indoor tanks.

2.3 Testing Equipment

The testing for the system is situated in Solar Lab, Singer 501. For this project, Solar Lab facilities were renovated and used as systems for testing the functionalities of the back-panel mount design. These facilities include a Q.PEAK DUO BLK-G8+ 340 Monocrystalline silicon module PV panel, a Prostar PWM-30M solar charge controller for power maximization and PV panel power monitoring, a Seahawk deepcycle battery as a load for the panel output, and a solar thermal fluid circulation and data acquisition system consisting of various pumps, valves, and associated sensors.

Figure 5. Q.PEAK DUO BLK-G8+ 340 PV module.

Figure 6. Battery and Prostar solar charge controller.

A schematic of the solar thermal fluid circulation and data acquisition system is shown in Fig. 7. The various valves and pumps allow circulating fluid to be pushed from one tank out to some test panel and back into the reservoir or either tank. Resistance temperature detectors (RTDs) were planted into tanks A and B and the inlets and outlets of the test panel measured the temperatures of liquids in the tanks and flows into and out of the panel. The system communicates with the MATLAB software on a desktop computer through the NI control box. Relays were used for transmitting signals of opening and closing valves and pumps, RTD transducers allowed RTD readings to be collected, and a flow meter signal amplifier passed the amplified flow meter signals in the form of pulses to the computer for further pulse detection and analysis.

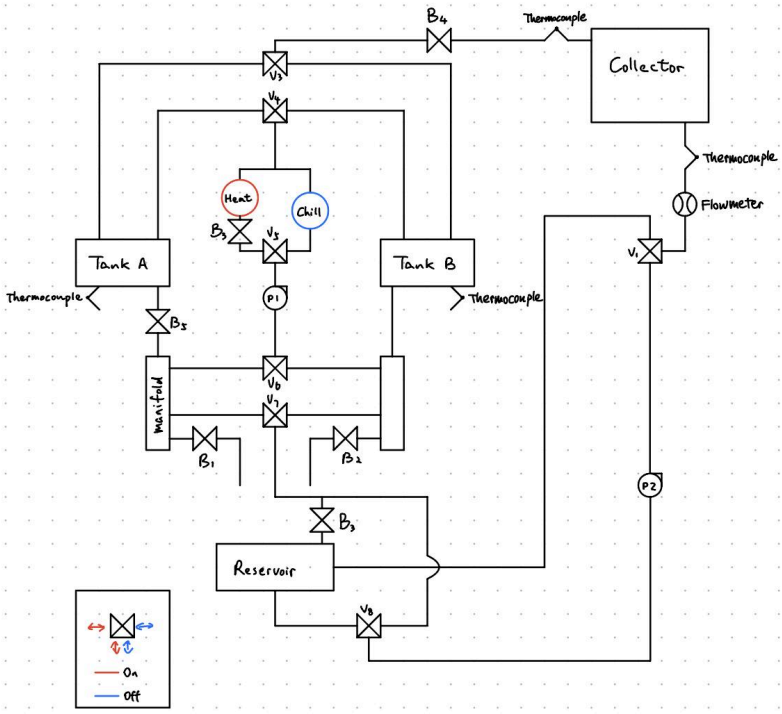

Figure 7. Schematic of the solar thermal fluid circulation system.

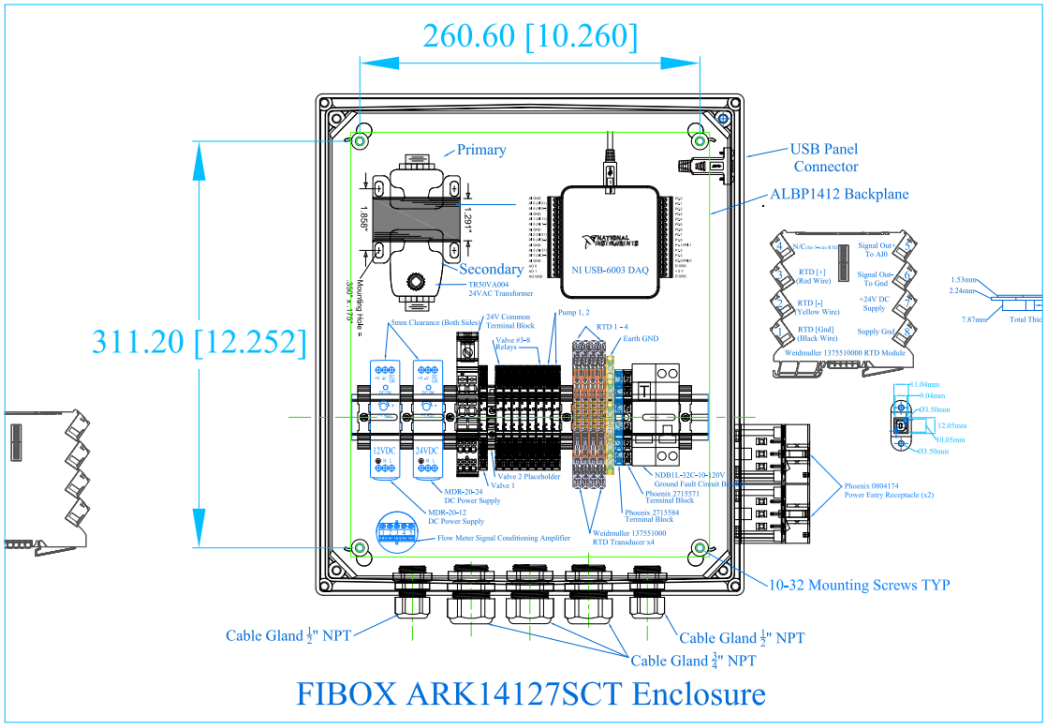

(a)

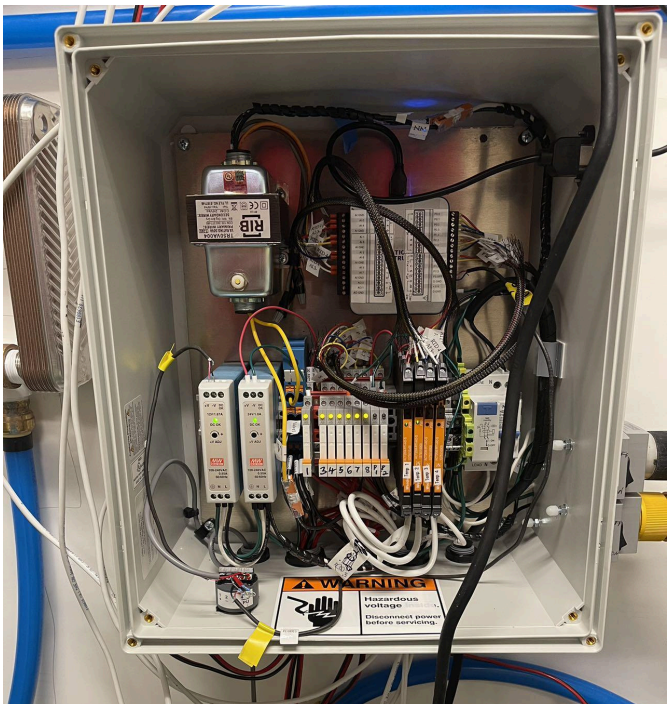

(b)

Figure 8. (a) Schematic and (b) photo of the solar thermal control box.

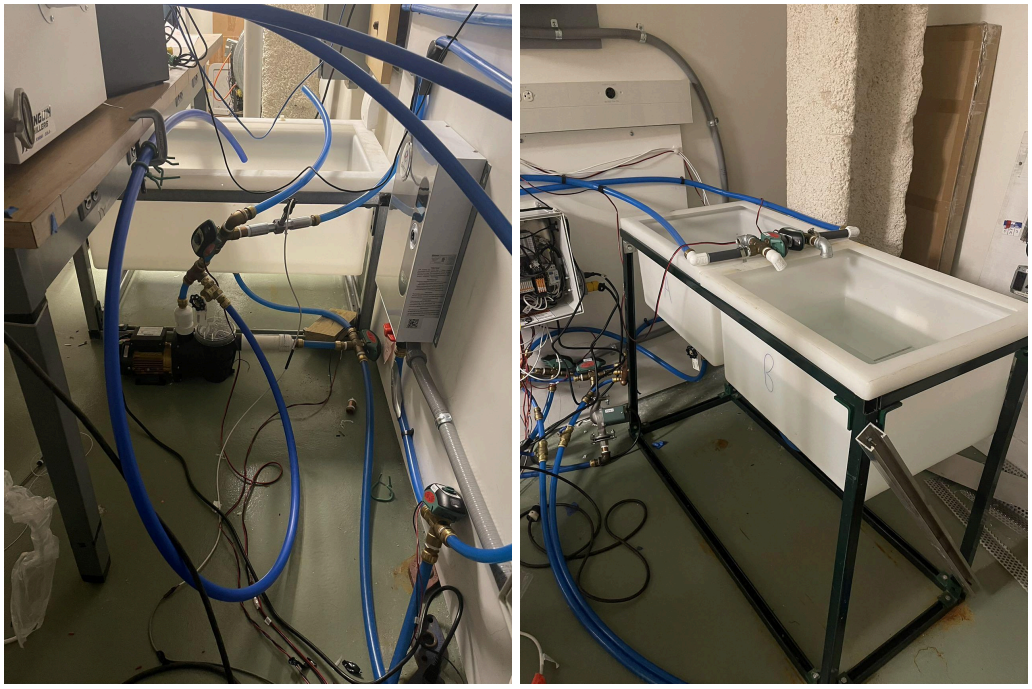

Figure 9. Pictures of the solar thermal fluid circulation system.

2.5 Testing Process

The mount was tested on a bright, cloudless, sunny, and warm day in late April. It lasted from 2:16 to 2:48 PM, such that there was a consistent irradiation on the PV panel for comparison of results. Each trial took 30 seconds with data taken at a five-second interval. Flow rate, water temperature, PV current, and PV voltage were taken in automated processes, while the panel temperature was taken manually. A photo of the testing setup during testing is shown in Fig. 9. The gathered data was then compiled into graphs relating PV power to panel temperature, panel temperature to mass flow rate, temperature difference to mass flow rate, and heat transfer rate to mass flow rate.

Figure 10. Setup during the testing process.

3. Results

The figures below show various trends that were observed from the data collected during the testing phase of this project.

Fig. 11 shows a roughly decreasing PV power as the panel temperature increases. The maximum difference, ignoring extreme values, between the PV power at maximum and minimum temperature is around 20 Watts.

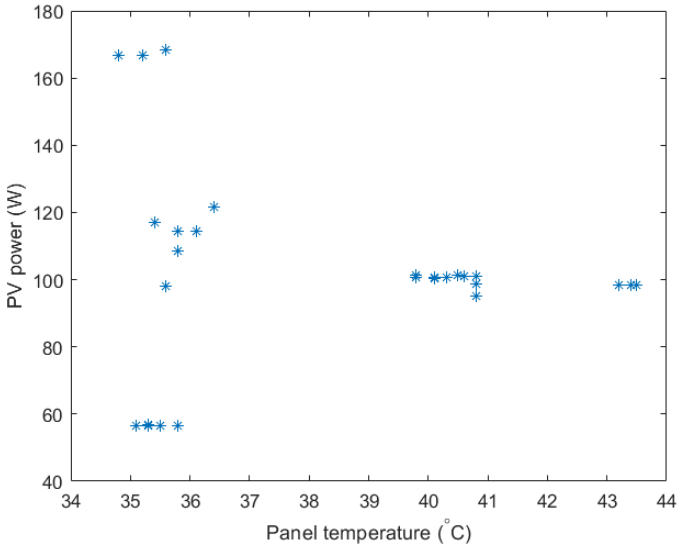

Figure 11. Graph of PV power plotted against panel temperature.

Fig. 12 shows a decreasing trend of panel temperature as the mass flow rate increases. There is a maximum of around 6 ℃ drop in panel temperature.

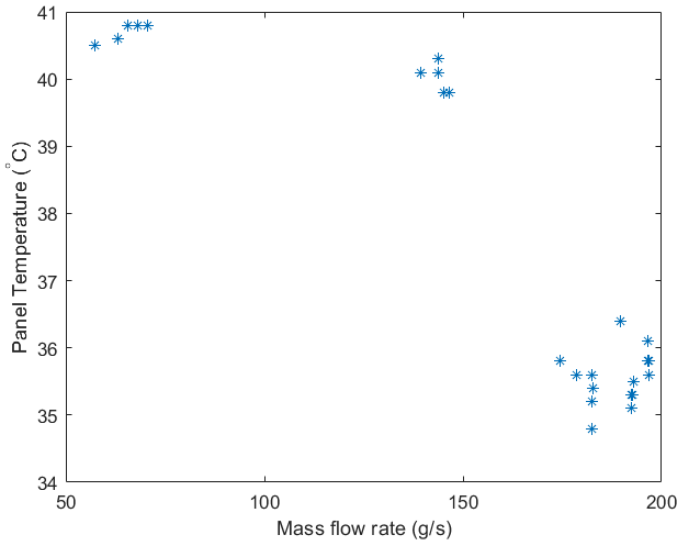

Figure 12. Graph of panel temperature plotted against mass flow rate of the cooling water.

Fig. 13 shows the temperature difference between the inlet and outlet of copper cooling tubing plotted against the mass flow rate. There is a negatively proportional relationship between the two variables, and the maximum temperature difference between the inlet and outlet is around 4 ℃.

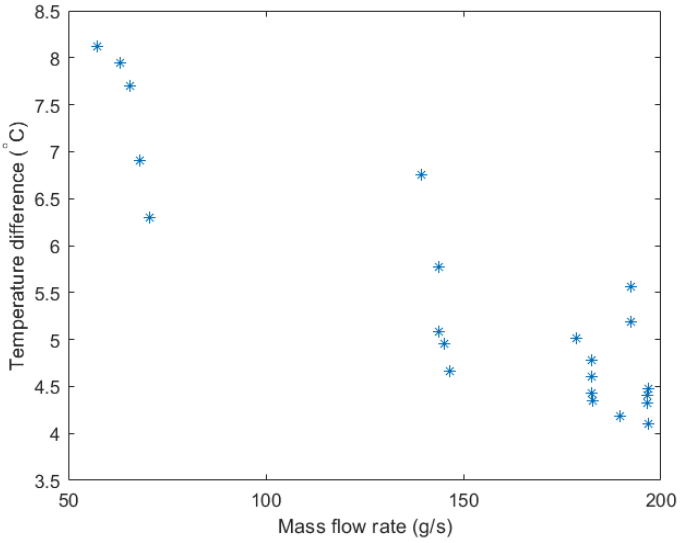

Figure 13. Graph of the temperature difference between the inlet and outlet of copper cooling tubing plotted against mass flow rate.

Fig. 14 shows the heat transfer rate calculated from the temperature difference between the inlet and outlet plotted against the mass flow rate. There is a nearly proportional relationship between the two variables.

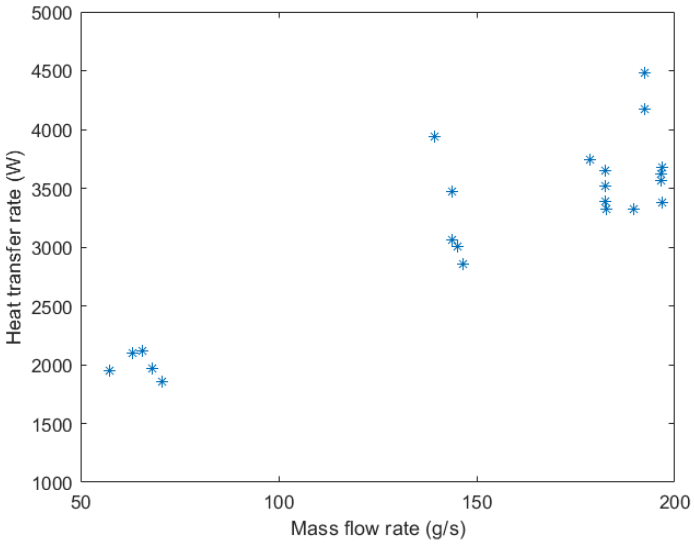

Figure 14. Graph of heat transfer rate calculated from the temperature difference between inlet and outlet plotted against mass flow rate.

4. Discussion

The results obtained from the testing phase of the project, as shown in the Results section, indicate some trends but are not conclusive due to insufficient data. Hence, an analysis of the present results is needed to make suggestions for future efforts.

4.1 Analysis of General Results

The data obtained from the test included a variety of data points at various temperatures, showing that the system operates at a relatively low temperature and small temperature difference, with a maximum panel temperature of less than 41℃ and a maximum panel temperature drop of 6 ℃, starts to experience a significant decrease in PV panel temperature and induce a reasonable increase in electrical output of around 20 Watts. However, they do not produce fully conclusive trends.

For PV power to panel temperature, there are outliers at the lower temperatures both at high and low PV powers. These might have occurred due to an incorrect temperature reading that may have occurred because the thermocouple was put too close to the copper tubing, which may have resulted in a measurement of the temperature of the tubing instead of the actual panel. A more thorough investigation into the cause would require more data taken over more diverse temperature ranges such that a more distinct trend can be observed.

Due to relatively cool ambient temperatures, the effectiveness of the heat transfer is not as large as estimated despite the very significant rise in the heat transfer rate. With a greater panel temperature that could go up to more than 50 ℃, as with the results obtained from my past summer research, the heat transfer rate may drastically increase along with the temperature difference between inlet and outlet. This calls for a more thorough analysis of the temperature distribution throughout the panel. With a more evenly distributed temperature, the efficiency of the system may further increase.

4.2 Future Outlook

Various constraints limit the materials used and the degree to which the system was controlled and optimized. Due to limitations in time, the downsizing of the system was not complete, a thorough evaluation of the system was not possible, and the design goals of the

system have not been met. In addition, more testing is needed to evaluate the full functionality of the system. Future work is needed to consider and remove some of these limiting factors.

This project evaluated various potential methods of channeling water along the back of the PV panel. The initial idea of cutting ducts out of foam material was not adopted, as foam materials that were tested easily broke down when exposed to flowing water. For the present design with s-shaped soft copper tubing, there is a limit to the bending radius. A design with a ladder-shaped scheme would have offered more thermal contact and better cooling, as copper tubing could be packed into a more compact scheme, allowing for more thermal contact. In addition, as the tubing in this scheme would not have undergone much shaping, the material would remain soft and could undergo flattening more easily, which also increases contact area. The temperature distribution across the panel would also be more even due to an even spread of channels instead of a single tubing.

More testing is recommended for hotter ambient temperatures with more direct sunlight during mid-summer, such as July or August. During this period, the maximum effectiveness of the heat transfer can be estimated more accurately, and the maximum efficiency of the system would be achieved.

In terms of further refining the present system, it is beneficial to implement a cooling loop into the present fluid circulation system in the testing mechanism to allow for a fully automated data collection process. With the fluid going into the panel put into thermal contact with a pump-powered circulation of cooling fluid through a chiller, one could potentially have the system running fluid from one tank out to the panel and back into that same tank without worrying about the tank running dry, which provides a better testing condition as a whole. With a cooling loop in the system, one could also implement a closed-loop cooling system, for which the circulation pump could be replaced with a pump with far lower power. Then, an analysis of the efficiency of the system would be possible. Since the system is presently operating with a powerful pump in an open loop, such evaluations would not show the true efficiency of a complete system.

With the complete system in place, more design can be implemented to meet the design goals:

1. An analysis of the proposed metric, η_{ht}, can be done.

2. More thorough temperature control can be completed through pumps with variable flow rate that control the circulation and cooling loop.
3. The system's control can be transferred to a microcontroller that can be assessed in terms of power consumption, where it is possible to reduce power consumption of the system via the microcontroller's sleep mode during times when cooling is not necessary.

A cost-benefit analysis can be done on the completed system in addition to the efficiency of the system in the proposed metrics. The cost of implementing a back-panel cooling system should be considered an initial cost of a PV panel in an analysis that compares the cost of producing electrical power in the lifespan of the PV panel with the cost of sourcing that electricity from the power grid. The pre-heated water is a source of cost-deduction, where the deducted cost can be determined from the cost of using a heater of the user's choice to generate the same amount of total energy in the volume of water.

5. Conclusion

The system operating at a relatively low temperature and small temperature difference, with a maximum panel temperature of less than 41℃ and a maximum panel temperature drop of 6 ℃, starts to experience a significant decrease in PV panel temperature and induce a reasonable increase in electrical output. Because of relatively cool ambient temperatures, the effectiveness of the heat transfer is not as large as estimated, and more experiments are recommended during mid-summer for a better understanding of the system. Future efforts should focus on increasing the thermal contact area, downsizing the system, and closing the circulation loop to generate conclusive results on system efficiency and cost-benefit evaluation.

6. Acknowledgement

I would like to express my deepest gratitude to Professor Carr Everbach for helping me along the entire project, Edmond Jaudi for installing and providing documentation and support for the Solar Control Box, and J. Johnson for helping me with the various aspects involved in the mechanics of copper tubing. Special thanks to the E14 students who helped to calibrate the flow

meter. I would also like to acknowledge the help of all who have supported me along the way and Swarthmore's engineering department for making this project possible.

7. References

Neamen, Donald. *Semiconductor Physics and Devices*. McGraw-Hill Science/Engineering/Math, 2003, books.google.ie/books?id=TPE9AQAAIAAJ&q=semiconductor+physics+and+devices&dq=semiconductor+physics+and+devices&hl=&cd=1&source=gbs_api.

Photovoltaics and Electricity - U.S. Energy Information Administration (EIA). www.eia.gov/energyexplained/solar/photovoltaics-and-electricity.php.

Moharram, K. A., et al. "Enhancing the Performance of Photovoltaic Panels by Water Cooling." *Ain Shams Engineering Journal*, vol. 869–877, no. 4, 1 Dec. 2013, https://doi.org/10.1016/j.asej.2013.03.005.

"Photovoltaic Energy Factsheet." *Center for Sustainable Systems*, css.umich.edu/publications/factsheets/energy/photovoltaic-energy-factsheet.

Duffie, John A., et al. *Solar Engineering of Thermal Processes, Photovoltaics and Wind*. John Wiley and Sons, 2020, books.google.ie/books?id=4vXPDwAAQBAJ&printsec=frontcover&dq=Solar+Engineering+of+Thermal+Processes,+Photovoltaics+and+Wind&hl=&cd=2&source=gbs_api.

Appendix I: Example MATLAB code for fluid circulation system startup

```
% program solar_thermal_init.m
% Data acquisition program for the thermal panel (North) side of the
% Singer Solar Lab. Initializes the values, pumps, and flowmeter
% last modified 26 April 2024
% To run individual sections, use Ctrl+Enter
clear
clf
dev = daqlist("ni")
warning off % turn off unnecessary warnings

s = daq("ni"); %s = daq.createSession('ni');
s.Rate = 10000; % set sample rate to 10000 samples/sec
ch0 = addinput(s,"Dev1", "ai0", "Voltage"); % Channel 0 for RTD 1
ch1 = addinput(s,"Dev1", "ai1", "Voltage"); % Channel 1 for RTD 2
ch2 = addinput(s,"Dev1", "ai2", "Voltage"); % Channel 2 for RTD 3
ch3 = addinput(s,"Dev1", "ai3", "Voltage"); % Channel 3 for RTD 4
ch0.TerminalConfig = "Differential"; % default is differential
ch1.TerminalConfig = "Differential"; % default is differential
ch2.TerminalConfig = "Differential"; % default is differential
ch3.TerminalConfig = "Differential"; % default is differential

d = daq("ni"); % for digital i/o channel
dq = addbidirectional(d,"Dev1","port0/line0","Digital"); % valve 1
dq.Direction = "Output"; % set output bit
dq = addbidirectional(d,"Dev1","port0/line1","Digital"); % no valve 2
dq.Direction = "Output"; % set output bit
dq = addbidirectional(d,"Dev1","port0/line2","Digital"); % valve 3
dq.Direction = "Output"; % set output bit
dq = addbidirectional(d,"Dev1","port0/line3","Digital"); % valve 4
dq.Direction = "Output"; % set output bit
dq = addbidirectional(d,"Dev1","port0/line4","Digital"); % valve 5
dq.Direction = "Output"; % set output bit
dq = addbidirectional(d,"Dev1","port0/line5","Digital"); % valve 6
dq.Direction = "Output"; % set output bit
dq = addbidirectional(d,"Dev1","port0/line6","Digital"); % valve 7
dq.Direction = "Output"; % set output bit
dq = addbidirectional(d,"Dev1","port0/line7","Digital"); % valve 8
dq.Direction = "Output"; % set output bit

p = daq("ni"); % for digital i/o line for pumps
dp = addbidirectional(p,"Dev1","port1/line0","Digital"); % pump 1
dp.Direction = "Output"; % set output bit
dp = addbidirectional(p,"Dev1","port1/line1","Digital"); % pump 2
dp.Direction = "Output"; % set output bit

flow = daq("ni"); % for counter i/o line for flowmeter
addinput(flow, "Dev1", "ctr0", "EdgeCount"); % set input properties

%% Test valves
write(d,[1 0 1 1 1 1 1 1]); % raise digital line high to activate valves
%% Read temperature
inst_temp = s.read
```

```
%% Run from reservoir to B
write(d,[1 0 0 0 0 0 0 1]); % raise digital line high to activate valves
%% Run from B to B
write(d,[1 0 0 0 0 0 1 0]);
%% Run from B to A
write(d,[1 0 1 0 0 0 1 0]);
%% Run from A to B
write(d,[1 0 0 0 0 0 0 0]);
%% Stop pump
write(p,[0 0]);
%% Turn off all valves
write(d,[0 0 0 0 0 0 0 0]);
%% Start pump
write(p,[0 1]);
%% Flowmeter reading
% Currently reads data every 5 seconds for 1 minute
total_duration = 0;
start_time = datetime('now');

num_data = 12;
flowdata = zeros(num_data,11);

counts = 0;
counts_prev = 0;
for i = 1:num_data
    sec = 0;
    t1 = datevec(datetime('now'));
    resetcounters(flow);
    counts_prev = read(flow).Dev1_ctr0;
    while sec < 5
        t2 = datevec(datetime('now'));
        % Turn into integer to compare to eliminate accumulated error when
        % using double
        if t2(6) < 10 && t1(6) >= 50
            sec = int8(t2)-int8(t1)+60;
        else
            sec = int8(t2)-int8(t1);
        end
    end
    temp = timetable2table(read(s));
    temp_vec = [temp.Dev1_ai0,temp.Dev1_ai1,temp.Dev1_ai2,temp.Dev1_ai3];
    counts = read(flow).Dev1_ctr0;
    flowdata(i,:) = [t2,counts-counts_prev,temp_vec];
    total_duration = total_duration + sec;
    resetcounters(flow);
end
```

Appendix II: Raw data sheets

Table 1. Raw PV voltage and current data.

Year	Month	Date	Hour	Minute	Second	Prostar PWM Array Voltage (V)	Prostar PWM Load Voltage (V)	Prostar PWM Charge Current (A)	Prostar PWM Battery Sense Voltage (V)	Prostar PWM LED State
2024	5	2	14	10	20	13.66	13.63	7.05	13.59	Green
2024	5	2	14	10	30	13.66	13.63	7.05	13.59	Green
2024	5	2	14	10	40	13.66	13.63	7.02	13.59	Green
2024	5	2	14	10	50	13.66	13.63	7.01	13.59	Green
2024	5	2	14	11	0	13.66	13.63	7.01	13.59	Green
2024	5	2	14	11	10	13.66	13.63	7.02	13.59	Green
2024	5	2	14	11	20	13.66	13.63	7.02	13.59	Green
2024	5	2	14	11	30	13.66	13.63	7.03	13.59	Green
2024	5	2	14	11	40	13.66	13.63	7.01	13.59	Green
2024	5	2	14	11	50	13.66	13.63	7.01	13.59	Green
2024	5	2	14	12	0	13.66	13.64	7.06	13.6	Green
2024	5	2	14	12	10	13.66	13.64	7.08	13.6	Green
2024	5	2	14	12	20	13.66	13.64	7.08	13.6	Green
2024	5	2	14	12	30	13.67	13.65	7.1	13.6	Green
2024	5	2	14	12	40	13.67	13.65	7.11	13.61	Green
2024	5	2	14	12	50	13.67	13.65	7.11	13.61	Green
2024	5	2	14	13	0	13.67	13.65	7.12	13.61	Green
2024	5	2	14	13	10	13.68	13.66	7.14	13.61	Green
2024	5	2	14	13	20	13.68	13.66	7.14	13.61	Green
2024	5	2	14	13	30	13.68	13.66	7.15	13.61	Green
2024	5	2	14	13	40	13.68	13.66	7.15	13.61	Green
2024	5	2	14	13	50	13.67	13.65	7.05	13.61	Green
2024	5	2	14	14	0	13.68	13.66	7.17	13.62	Green
2024	5	2	14	14	10	13.68	13.66	7.17	13.62	Green
2024	5	2	14	14	20	13.69	13.66	7.18	13.62	Green
2024	5	2	14	14	30	13.69	13.66	7.19	13.62	Green
2024	5	2	14	14	40	13.69	13.66	7.19	13.62	Green
2024	5	2	14	14	50	13.69	13.66	7.19	13.63	Green
2024	5	2	14	15	0	13.69	13.66	7.19	13.63	Green
2024	5	2	14	15	10	13.69	13.66	7.19	13.63	Green
2024	5	2	14	15	20	13.7	13.66	7.16	13.63	Green
2024	5	2	14	15	30	13.7	13.66	7.17	13.63	Green
2024	5	2	14	15	40	13.7	13.66	7.17	13.63	Green
2024	5	2	14	15	50	13.7	13.66	7.17	13.63	Green
2024	5	2	14	16	0	13.7	13.67	7.19	13.63	Green
2024	5	2	14	16	10	13.7	13.67	7.19	13.63	Green
2024	5	2	14	16	20	13.7	13.67	7.2	13.63	Green
2024	5	2	14	16	30	13.7	13.67	7.2	13.63	Green
2024	5	2	14	16	40	13.7	13.67	7.17	13.63	Green
2024	5	2	14	16	50	13.7	13.67	7.17	13.63	Green
2024	5	2	14	17	0	13.7	13.67	7.17	13.63	Green
2024	5	2	14	17	10	13.7	13.67	7.17	13.63	Green
2024	5	2	14	17	20	13.7	13.67	7.14	13.63	Green
2024	5	2	14	17	30	13.7	13.67	7.14	13.63	Green
2024	5	2	14	17	40	13.7	13.67	7.16	13.63	Green

2024	5	2	14	17	50	13.7	13.67	7.1	13.63	Green
2024	5	2	14	18	0	13.7	13.67	7.1	13.63	Green
2024	5	2	14	18	10	13.7	13.67	7.14	13.63	Green
2024	5	2	14	18	20	13.7	13.67	7.11	13.63	Green
2024	5	2	14	18	30	13.7	13.67	7.11	13.63	Green
2024	5	2	14	18	40	13.7	13.68	7.13	13.63	Green
2024	5	2	14	18	50	13.7	13.68	7.13	13.63	Green
2024	5	2	14	19	0	13.7	13.68	7.15	13.63	Green
2024	5	2	14	19	10	13.71	13.69	7.21	13.64	Green
2024	5	2	14	19	20	13.71	13.69	7.21	13.64	Green
2024	5	2	14	19	30	13.71	13.69	7.25	13.65	Green
2024	5	2	14	19	40	13.72	13.7	7.3	13.65	Green
2024	5	2	14	19	50	13.72	13.7	7.3	13.65	Green
2024	5	2	14	20	0	13.73	13.7	7.32	13.66	Green
2024	5	2	14	20	10	13.73	13.7	7.34	13.66	Green
2024	5	2	14	20	20	13.73	13.7	7.34	13.66	Green
2024	5	2	14	20	30	13.73	13.7	7.38	13.66	Green
2024	5	2	14	20	40	13.73	13.7	7.34	13.66	Green
2024	5	2	14	20	50	13.73	13.7	7.34	13.66	Green
2024	5	2	14	21	0	13.73	13.71	7.32	13.66	Green
2024	5	2	14	21	10	13.73	13.71	7.32	13.66	Green
2024	5	2	14	21	20	13.73	13.71	7.32	13.66	Green
2024	5	2	14	21	30	13.73	13.71	7.31	13.66	Green
2024	5	2	14	21	40	13.73	13.71	7.31	13.66	Green
2024	5	2	14	21	50	13.73	13.71	7.31	13.66	Green
2024	5	2	14	22	0	13.74	13.72	7.41	13.67	Green
2024	5	2	14	22	10	13.74	13.72	7.41	13.67	Green
2024	5	2	14	22	20	13.74	13.72	7.4	13.67	Green
2024	5	2	14	22	30	13.75	13.72	7.42	13.68	Green
2024	5	2	14	22	40	13.75	13.72	7.42	13.68	Green
2024	5	2	14	22	50	13.75	13.73	7.42	13.68	Green
2024	5	2	14	23	0	13.75	13.73	7.42	13.68	Green
2024	5	2	14	23	10	13.75	13.73	7.42	13.68	Green
2024	5	2	14	23	20	13.76	13.73	7.41	13.69	Green
2024	5	2	14	23	30	13.75	13.73	7.41	13.69	Green
2024	5	2	14	23	40	13.75	13.73	7.41	13.69	Green
2024	5	2	14	23	50	13.76	13.73	7.45	13.69	Green
2024	5	2	14	24	0	13.76	13.73	7.46	13.69	Green
2024	5	2	14	24	10	13.76	13.73	7.46	13.69	Green
2024	5	2	14	24	20	13.77	13.73	7.47	13.69	Green
2024	5	2	14	24	30	13.77	13.73	7.47	13.69	Green
2024	5	2	14	24	40	13.76	13.73	7.36	13.69	Green
2024	5	2	14	24	50	13.76	13.73	7.33	13.69	Green
2024	5	2	14	25	0	13.76	13.73	7.33	13.69	Green
2024	5	2	14	25	10	13.74	13.72	7.19	13.68	Green
2024	5	2	14	25	20	13.73	13.7	6.93	13.66	Green
2024	5	2	14	25	30	13.73	13.7	6.93	13.66	Green
2024	5	2	14	25	40	13.71	13.7	6.8	13.65	Green
2024	5	2	14	25	50	13.71	13.7	6.83	13.65	Green
2024	5	2	14	26	0	13.71	13.7	6.83	13.65	Green
2024	5	2	14	26	10	13.71	13.7	6.89	13.65	Green
2024	5	2	14	26	20	13.7	13.68	6.77	13.65	Green
2024	5	2	14	26	30	13.7	13.68	6.77	13.65	Green
2024	5	2	14	26	40	13.68	13.66	6.26	13.63	Green
2024	5	2	14	26	50	13.68	13.66	6.26	13.63	Green
2024	5	2	14	27	0	13.66	13.64	6.06	13.6	Green

2024	5	2	14	27	10	13.69	13.66	6.6	13.63	Green
2024	5	2	14	27	20	13.69	13.66	6.6	13.63	Green
2024	5	2	14	27	30	13.7	13.68	6.96	13.66	Green
2024	5	2	14	27	40	13.71	13.7	6.89	13.65	Green
2024	5	2	14	27	50	13.71	13.7	6.89	13.65	Green
2024	5	2	14	28	0	13.73	13.71	7.16	13.67	Green
2024	5	2	14	28	10	13.75	13.73	7.3	13.69	Green
2024	5	2	14	28	20	13.75	13.73	7.3	13.69	Green
2024	5	2	14	28	30	13.77	13.74	7.44	13.7	Green
2024	5	2	14	28	40	13.79	13.76	7.7	13.72	Green
2024	5	2	14	28	50	13.79	13.76	7.7	13.72	Green
2024	5	2	14	29	0	13.8	13.77	7.71	13.73	Green
2024	5	2	14	29	10	13.79	13.77	7.54	13.72	Green
2024	5	2	14	29	20	13.79	13.77	7.54	13.72	Green
2024	5	2	14	29	30	13.8	13.77	7.52	13.73	Green
2024	5	2	14	29	40	13.8	13.77	7.52	13.73	Green
2024	5	2	14	29	50	13.82	13.79	7.81	13.74	Green
2024	5	2	14	30	0	13.84	13.8	8.02	13.77	Green
2024	5	2	14	30	10	13.84	13.8	8.02	13.77	Green
2024	5	2	14	30	20	13.85	13.81	8.09	13.77	Green
2024	5	2	14	30	30	13.86	13.83	8.14	13.78	Green
2024	5	2	14	30	40	13.86	13.83	8.14	13.78	Green
2024	5	2	14	30	50	13.87	13.83	8.16	13.79	Green
2024	5	2	14	31	0	13.88	13.84	8.37	13.8	Green
2024	5	2	14	31	10	13.88	13.84	8.37	13.8	Green
2024	5	2	14	31	20	13.9	13.87	8.52	13.82	Green
2024	5	2	14	31	30	13.91	13.88	8.66	13.84	Green
2024	5	2	14	31	40	13.91	13.88	8.66	13.84	Green
2024	5	2	14	31	50	13.92	13.88	8.63	13.84	Green
2024	5	2	14	32	0	13.92	13.88	8.63	13.84	Green
2024	5	2	14	32	10	13.91	13.87	8.42	13.83	Green
2024	5	2	14	32	20	13.94	13.89	8.71	13.85	Green
2024	5	2	14	32	30	13.94	13.89	8.71	13.85	Green
2024	5	2	14	32	40	13.94	13.9	8.73	13.85	Green
2024	5	2	14	32	50	13.91	13.88	8.23	13.83	Green
2024	5	2	14	33	0	13.91	13.88	8.23	13.83	Green
2024	5	2	14	33	10	13.88	13.84	7.82	13.8	Green
2024	5	2	14	33	20	13.81	13.79	7.09	13.75	Green
2024	5	2	14	33	30	13.81	13.79	7.09	13.75	Green
2024	5	2	14	33	40	13.76	13.74	6.55	13.7	Green
2024	5	2	14	33	50	13.73	13.72	6.33	13.67	Green
2024	5	2	14	34	0	13.73	13.72	6.33	13.67	Green
2024	5	2	14	34	10	13.74	13.73	6.61	13.68	Green
2024	5	2	14	34	20	13.73	13.71	6.41	13.66	Green
2024	5	2	14	34	30	13.73	13.71	6.41	13.66	Green
2024	5	2	14	34	40	13.66	13.65	5.23	13.58	Green
2024	5	2	14	34	50	13.66	13.65	5.23	13.58	Green
2024	5	2	14	35	0	13.72	13.7	6.89	13.69	Green
2024	5	2	14	35	10	13.8	13.77	7.52	13.73	Green
2024	5	2	14	35	20	13.8	13.77	7.52	13.73	Green
2024	5	2	14	35	30	13.8	13.77	7.1	13.71	Green
2024	5	2	14	35	40	13.73	13.72	6.44	13.68	Green
2024	5	2	14	35	50	13.73	13.72	6.44	13.68	Green
2024	5	2	14	36	0	13.72	13.71	6.19	13.65	Green
2024	5	2	14	36	10	13.71	13.7	6.48	13.67	Green
2024	5	2	14	36	20	13.71	13.7	6.48	13.67	Green

2024	5	2	14	36	30	13.77	13.75	7.38	13.73	Green
2024	5	2	14	36	40	13.82	13.8	7.69	13.76	Green
2024	5	2	14	36	50	13.82	13.8	7.69	13.76	Green
2024	5	2	14	37	0	13.81	13.79	7.45	13.74	Green
2024	5	2	14	37	10	13.81	13.79	7.45	13.74	Green
2024	5	2	14	37	20	13.8	13.78	6.95	13.71	Green
2024	5	2	14	37	30	13.92	13.88	8.66	13.84	Green
2024	5	2	14	37	40	13.92	13.88	8.66	13.84	Green
2024	5	2	14	37	50	13.95	13.91	8.79	13.85	Green
2024	5	2	14	38	0	13.87	13.84	7.55	13.81	Green
2024	5	2	14	38	10	13.87	13.84	7.55	13.81	Green
2024	5	2	14	38	20	13.91	13.88	8.28	13.84	Green
2024	5	2	14	38	30	13.98	13.94	8.91	13.86	Green
2024	5	2	14	38	40	13.98	13.94	8.91	13.86	Green
2024	5	2	14	38	50	13.8	13.78	6.57	13.75	Green
2024	5	2	14	39	0	13.67	13.67	4.81	13.62	Green
2024	5	2	14	39	10	13.67	13.67	4.81	13.62	Green
2024	5	2	14	39	20	13.64	13.63	4.98	13.6	Green
2024	5	2	14	39	30	13.6	13.61	4.69	13.55	Green
2024	5	2	14	39	40	13.6	13.61	4.69	13.55	Green
2024	5	2	14	39	50	13.57	13.58	4.57	13.54	Green
2024	5	2	14	40	0	13.57	13.58	4.57	13.54	Green
2024	5	2	14	40	10	13.57	13.57	4.72	13.53	Green
2024	5	2	14	40	20	13.88	13.84	9.16	13.78	Green
2024	5	2	14	40	30	13.88	13.84	9.16	13.78	Green
2024	5	2	14	40	40	13.73	13.72	6.64	13.67	Green
2024	5	2	14	40	50	13.73	13.71	6.32	13.72	Green
2024	5	2	14	41	0	13.73	13.71	6.32	13.72	Green
2024	5	2	14	41	10	13.96	13.91	9.43	13.91	Green
2024	5	2	14	41	20	14.02	13.97	9.45	13.92	Green
2024	5	2	14	41	30	14.02	13.97	9.45	13.92	Green
2024	5	2	14	41	40	15.31	14.05	10.64	13.95	Green
2024	5	2	14	41	50	13.96	13.92	8.44	13.91	Green
2024	5	2	14	42	0	13.96	13.92	8.44	13.91	Green
2024	5	2	14	42	10	13.69	13.69	4.61	13.64	Green
2024	5	2	14	42	20	13.69	13.69	4.61	13.64	Green
2024	5	2	14	42	30	13.88	13.84	8.73	13.81	Green
2024	5	2	14	42	40	13.6	13.61	4.28	13.57	Green
2024	5	2	14	42	50	13.6	13.61	4.28	13.57	Green
2024	5	2	14	43	0	13.59	13.59	4.34	13.54	Green
2024	5	2	14	43	10	13.55	13.55	4.13	13.52	Green
2024	5	2	14	43	20	13.55	13.55	4.13	13.52	Green
2024	5	2	14	43	30	13.53	13.54	4.24	13.51	Green
2024	5	2	14	43	40	13.55	13.55	4.17	13.52	Green
2024	5	2	14	43	50	13.55	13.55	4.17	13.52	Green
2024	5	2	14	44	0	13.53	13.54	4.21	13.5	Green
2024	5	2	14	44	10	13.52	13.54	4.18	13.49	Green
2024	5	2	14	44	20	13.52	13.54	4.18	13.49	Green
2024	5	2	14	44	30	13.5	13.52	4.04	13.48	Green
2024	5	2	14	44	40	13.5	13.52	4.04	13.48	Green
2024	5	2	14	44	50	13.63	13.62	5.87	13.57	Green
2024	5	2	14	45	0	13.58	13.58	4.87	13.52	Green
2024	5	2	14	45	10	13.58	13.58	4.87	13.52	Green
2024	5	2	14	45	20	13.51	13.52	4.04	13.48	Green
2024	5	2	14	45	30	13.88	13.84	9.75	13.84	Green
2024	5	2	14	45	40	13.88	13.84	9.75	13.84	Green

2024	5	2	14	45	50	13.99	13.95	9.74	13.88	Green
2024	5	2	14	46	0	13.66	13.66	5.25	13.63	Green
2024	5	2	14	46	10	13.66	13.66	5.25	13.63	Green
2024	5	2	14	46	20	13.59	13.6	4.08	13.57	Green
2024	5	2	14	46	30	14.02	13.98	9.38	13.77	Green
2024	5	2	14	46	40	14.02	13.98	9.38	13.77	Green
2024	5	2	14	46	50	13.7	13.7	4.98	13.6	Green
2024	5	2	14	47	0	14.05	14	10.37	13.95	Green
2024	5	2	14	47	10	14.05	14	10.37	13.95	Green
2024	5	2	14	47	20	14.09	14.02	9.7	13.97	Green
2024	5	2	14	47	30	14.09	14.02	9.7	13.97	Green
2024	5	2	14	47	40	15.95	14.05	10.3	13.95	Green
2024	5	2	14	47	50	16.5	14.07	10.21	13.96	Absorption (Flashing Green)
2024	5	2	14	48	0	16.5	14.07	10.21	13.96	Absorption (Flashing Green)
2024	5	2	14	48	10	14.19	14.01	8.25	13.87	Green
2024	5	2	14	48	20	16.19	14.06	10.3	13.96	Green
2024	5	2	14	48	30	16.19	14.06	10.3	13.96	Green
2024	5	2	14	48	40	13.96	13.93	8.01	13.91	Green
2024	5	2	14	48	50	13.77	13.77	4.82	13.7	Green
2024	5	2	14	49	0	13.77	13.77	4.82	13.7	Green
2024	5	2	14	15	30	13.7	13.66	7.17	13.63	Green
2024	5	2	14	15	40	13.7	13.66	7.17	13.63	Green
2024	5	2	14	15	50	13.7	13.66	7.17	13.63	Green
2024	5	2	14	16	0	13.7	13.67	7.19	13.63	Green
2024	5	2	14	16	10	13.7	13.67	7.19	13.63	Green
2024	5	2	14	16	20	13.7	13.67	7.2	13.63	Green

Below are tables of raw data for tests 2 to 6. Notice that the first test was done without flow to set a temperature ceiling and power output floor as a reference, as shown in the last six rows in Table 1.

Table 2. Raw solar thermal data for test 2.

Year	Month	Date	Hour	Minute	Second	Flow meter count	RTD1 reading	RTD2 reading	RTD3 reading	RTD4 reading
2024	5	2	14	19	59.50	2750	1.92	2.08	2.28	1.89
2024	5	2	14	20	9.50	2887	1.90	2.07	2.15	1.92
2024	5	2	14	20	14.50	2906	1.91	2.08	2.15	1.91
2024	5	2	14	20	19.50	2917	1.92	2.07	2.11	1.90
2024	5	2	14	20	24.50	2909	1.92	2.12	2.08	1.90
2024	5	2	14	20	29.50	2916	1.90	2.10	2.05	1.89
2024	5	2	14	20	34.50	2929	1.90	2.10	2.05	1.89
2024	5	2	14	20	39.50	2948	1.94	2.10	2.06	1.90
2024	5	2	14	20	44.50	2953	1.92	2.06	2.04	1.91
2024	5	2	14	20	49.50	2981	1.90	2.09	2.05	1.91

Table 3. Raw solar thermal data for test 3.

Year	Month	Date	Hour	Minute	Second	Flow meter count	RTD1 reading	RTD2 reading	RTD3 reading	RTD4 reading
2024	5	2	14	24	35.50	1034	1.89	1.97	2.35	1.95
2024	5	2	14	24	40.50	1226	1.90	1.96	2.34	1.89
2024	5	2	14	24	45.50	1220	1.88	1.96	2.29	1.90
2024	5	2	14	24	50.50	1276	1.92	1.95	2.31	1.88
2024	5	2	14	24	55.50	1263	1.89	1.95	2.30	1.88
2024	5	2	14	25	9.50	1339	1.88	1.96	2.25	1.88
2024	5	2	14	25	14.50	1322	1.86	2.00	2.20	1.88
2024	5	2	14	25	19.50	1382	1.90	1.97	2.21	1.88
2024	5	2	14	25	24.50	1389	1.89	1.99	2.14	1.90
2024	5	2	14	25	29.50	1417	1.87	1.94	2.18	1.88

Table 4. Raw solar thermal data for test 4.

Year	Month	Date	Hour	Minute	Second	Flow meter count	RTD1 reading	RTD2 reading	RTD3 reading	RTD4 reading
2024	5	2	14	32	33.50	3714	1.81	1.95	2.11	2.01
2024	5	2	14	32	38.50	3999	1.84	2.00	2.09	2.05
2024	5	2	14	32	43.50	3993	1.85	1.99	2.11	2.04
2024	5	2	14	32	48.50	3998	1.84	2.01	2.13	2.01
2024	5	2	14	32	53.50	3997	1.84	1.99	2.13	2.04
2024	5	2	14	32	58.50	3999	1.80	1.98	2.11	2.03
2024	5	2	14	33	9.50	4000	1.86	1.99	2.13	2.02
2024	5	2	14	33	14.50	4002	1.80	2.00	2.11	2.03
2024	5	2	14	33	19.50	4000	1.83	2.00	2.09	2.06
2024	5	2	14	33	24.50	4002	1.83	1.95	2.14	2.05

Table 5. Raw solar thermal data for test 5.

Year	Month	Date	Hour	Minute	Second	Flow meter count	RTD1 reading	RTD2 reading	RTD3 reading	RTD4 reading
2024	5	2	14	43	33.50	3156	1.84	2.07	2.81	2.11
2024	5	2	14	43	38.50	3930	1.81	2.07	2.91	2.06
2024	5	2	14	43	43.50	3923	1.81	2.08	3.18	2.07
2024	5	2	14	43	48.50	3920	1.84	2.08	3.11	2.03
2024	5	2	14	43	53.50	3918	1.85	2.08	2.63	2.02
2024	5	2	14	43	58.50	3914	1.84	2.09	2.38	1.99
2024	5	2	14	44	9.50	3912	1.86	2.22	2.23	2.04
2024	5	2	14	44	14.50	3912	1.81	2.39	2.23	2.04
2024	5	2	14	44	19.50	3911	1.79	2.50	2.22	2.02
2024	5	2	14	44	24.50	3908	1.84	2.57	2.16	2.03

Table 6. Raw solar thermal data for test 6.

Year	Month	Date	Hour	Minute	Second	Flow meter count	RTD1 reading	RTD2 reading	RTD3 reading	RTD4 reading
2024	5	2	14	47	47.50	3546	1.90	2.48	2.02	1.83
2024	5	2	14	47	52.50	3712	1.91	2.48	1.99	1.83
2024	5	2	14	47	57.50	3708	1.89	2.46	1.96	1.86
2024	5	2	14	48	9.50	3703	1.88	2.45	1.98	1.83
2024	5	2	14	48	14.50	3711	1.87	2.41	1.96	1.84
2024	5	2	14	48	19.50	3708	1.87	2.43	1.96	1.85
2024	5	2	14	48	24.50	3706	1.90	2.40	1.99	1.84
2024	5	2	14	48	29.50	3705	1.85	2.42	1.95	1.83
2024	5	2	14	48	34.50	3708	1.87	2.38	1.96	1.83
2024	5	2	14	48	39.50	3707	1.89	2.37	2.01	1.83

Appendix III: Flow meter and RTD calibrations

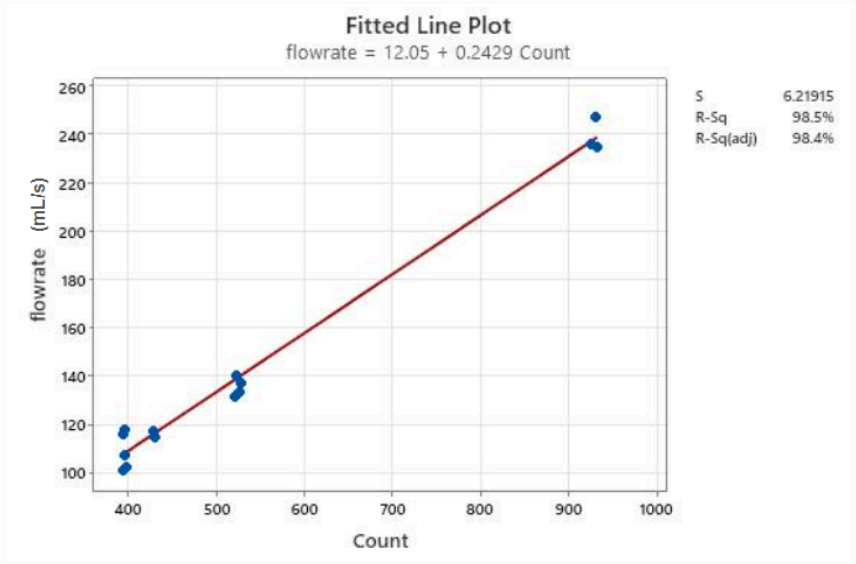

Figure 1. Flow meter calibration curve.

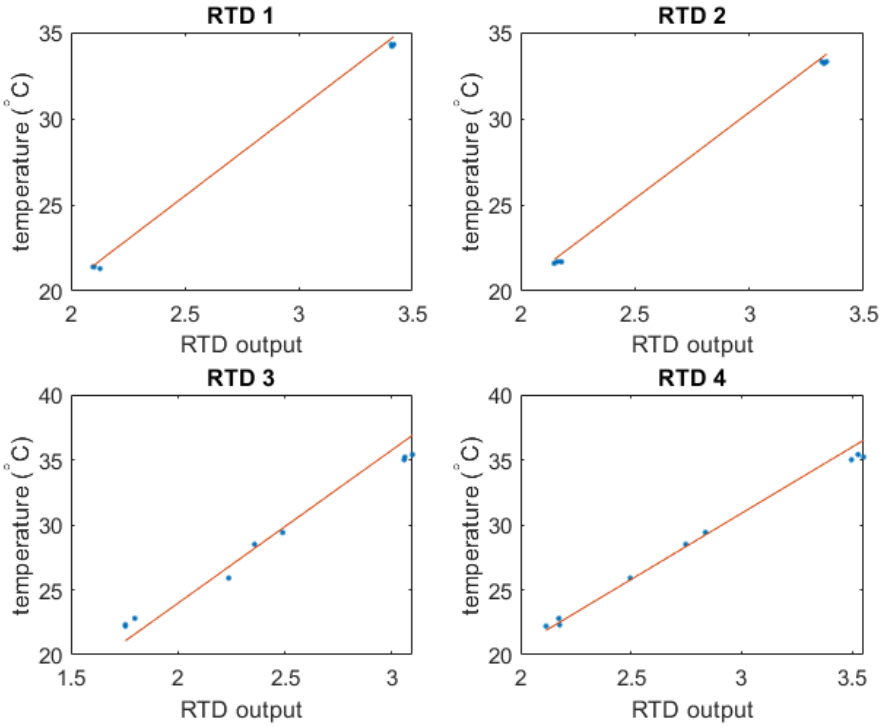

Figure 2. RTD calibration curves.

Table 2. Calibration matrices (in the form of y = b0 + b1*y).

flowmeter_calibration	[12.0500,0.2429]
rtd1_calibration	[0.3432,10.0674]
rtd2_calibration	[0.3486,10.0036]
rtd3_calibration	[0.3967,11.7833]
rtd4_calibration	[0.3439,10.1795]